

Magnetic Behaviors of Heterospin Chains Consisting of Cobalt(II) Complexes and Dipyridylcarbenes

Satoru Karasawa and Noboru Koga*

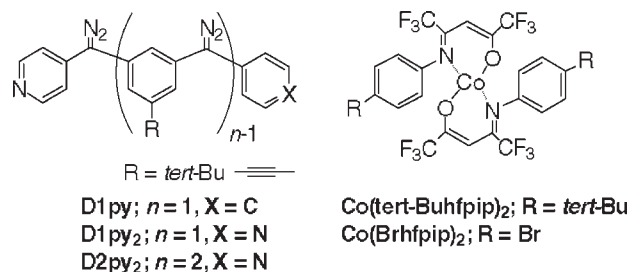
Graduate School of Pharmaceutical Sciences, Kyushu University, 3-1-1 Maidashi, Higashi-ku, Fukuoka, 812-8582 Japan

Supporting Information

ABSTRACT: The 1:1 mixture of $\text{Co}(\text{Brhfpip})_2$ and D1py_2 gave isomeric diazocobalt complexes, **1** and **2**, formulated by $[\text{Co}(\text{Brhfpip})_2(\text{D1py}_2)]_n$. Complexes **1** and **2** have zigzag and linear chain structures by the cis and trans coordination of pyridine units in D1py_2 , respectively. After irradiation of microcrystalline samples, the generated carbene interacted with the cobalt ion to form ferromagnetic chains, **1c** and **2c**. Those isomeric chains exhibited slow magnetic relaxation with $U_{\text{eff}} = 93$ and 87 K and $H_c = 20$ and 13 kOe at 1.9 K for **1c** and **2c**, respectively.

Heterospin systems¹ consisting of 3d spins of metal ions and 2p spins due to organic radicals and carbenes can provide unique molecule-based magnets by varying the combination of the chelating metal complexes (or metal ions) and the ligands carrying organic spins. The combination of the anisotropic cobalt(II) complexes (or ion) and diazomopyridine derivative, D1py , where the diazo moiety is a precursor for carbene, led to new types of single-molecule magnets (SMMs)² with a high effective activation barrier, U_{eff} , which corresponds to $|D|S^2$; D and S are the anisotropic parameter and the spin quantum number, for reorientation of the magnetic moment.³ When diazodipyridine derivatives, D1py_2 , were used as photoresponsive magnetic couplers,⁴ the formation of a high-spin polymeric chain after irradiation was expected. Actually, the combination of D1py_2 and isotropic metal complexes, Cu^{II} - and $\text{Mn}^{\text{II}}(\text{hfac})_2$ (hfac = hexafluoroacetylacetonato), was reported to provide ferro- and ferrimagnetic chains, respectively, after irradiation.^{4b,4c} In the combination of D1py_2 and anisotropic metal complexes, on the other hand, the low efficiency of photolysis in the solid state prevented investigation of their magnetic properties. A magnetic unianisotropic chain is known as a single-chain magnet (SCM).⁵ The activation barrier, Δ_{eff} , for SCM is expressed as the summation of a correlation length energy, $\Delta_1 (=4JS^2$; J is the exchange coupling parameter), and an anisotropic energy, $\Delta_a (=|D|S^2)$ in a finite-length region of the Ising model. Recently, it was found that a cyclic dinuclear cobalt(II) complex, $[\text{Co}(\text{tert-Buhfpip})_2(\text{D2py}_2)]_2$, was photolyzed in the crystalline state to form an SMM with $U_{\text{eff}} = 96$ K.⁶ The finding that photolysis of the diazoCo-(hfpip)₂ complex in the crystalline state effectively took place allows application of the heterospin system to the study of

polymetallic chains. In this study, D1py_2 was used, and 1:1 polymeric complexes of $\text{Co}(\text{Brhfpip})_2$ with D1py_2 having zigzag and linear chain structures were successfully prepared. We report here the crystal structure of cobalt(II) complexes composed of D1py_2 and $\text{Co}(\text{Brhfpip})_2$ and their magnetic behaviors before and after irradiation.



The solutions of D1py_2 and $\text{Co}(\text{Brhfpip})_2$ ⁷ were mixed at a 1:1 ratio under different conditions (I and II in S1 in the Supporting Information, SI) to afford two single crystals of 1:1 cobalt(II) complexes, **1** and **2**, formulated by $[\text{Co}(\text{Brhfpip})_2(\text{D1py}_2)]_n$ independently as dark orange chips and platelets, respectively. The selective recrystallizations for **1** and **2** were reproducible. The molecular structures of **1** and **2** revealed by X-ray crystallography are shown in Figure 1. In both complexes, **1** has a center of symmetry between the chains, while **2** has two centers of symmetry at the cobalt ions within the chain. The ligand D1py_2 coordinated to $\text{Co}(\text{Brhfpip})_2$ in cis and trans configurations, forming zigzag and linear chains for **1** and **2**, respectively. The cobalt ion units have compressed octahedral structures, in which the bond lengths between the cobalt ion and the axial ligands are 2.023 ($r_{\text{Co}-\text{O}_1}$) and 2.026 ($r_{\text{Co}-\text{O}_2}$) Å for **1** and 2.008 ($r_{\text{Co}_1-\text{O}}$) and 2.021 ($r_{\text{Co}_2-\text{O}}$) Å for **2**. These are shorter by 0.18–0.20 Å for **1** and 0.13–0.22 Å for **2** compared with those for $r_{\text{Co}-\text{N}}$. The dihedral angles (py–py) between the pyridine planes in the D1py_2 unit are 36.4° for **1** and 31.3° for **2**, suggesting that the generated carbene spin after photolysis of diazo moieties effectively delocalized in both pyridine rings. The dihedral angles (py–xy) between the pyridine plane and the X–Y plane defined by four nitrogen atoms coordinating to the cobalt ion are 70.2 and 73.1° for **1**. On the other hand, in **2**, two kinds of cobalt pyridine units, A and B, having py–xy of 77.7 and 48.0°, respectively, existed alternately in the chain (Figure 1b). The observed difference in dihedral angles for units A and B might affect the magnetic exchange couplings between the cobalt

Received: November 20, 2010

Published: January 31, 2011

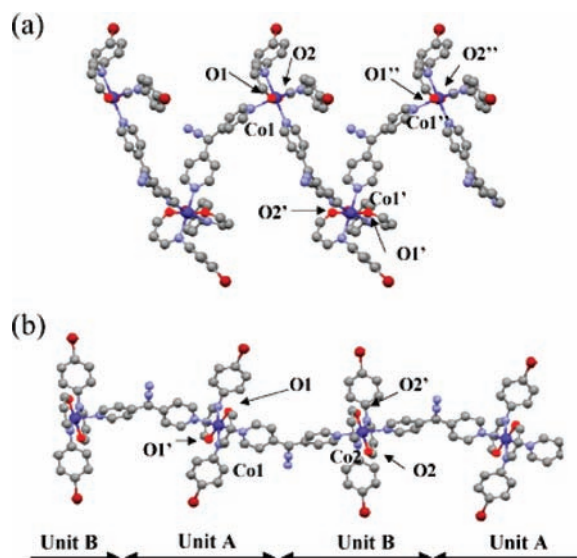


Figure 1. Molecular structures of **1** (a) and **2** (b), represented by a ball-and-stick model (color code: cobalt, blue; carbon, gray; oxygen, red; nitrogen, light blue; bromine, wine red). Hydrogen atoms and trifluoromethyl groups are omitted for the sake of clarity.

ion and the generated carbene. The distances between the cobalt ions within the chain are 11.6 and 14.0 Å in **1** and 12.0 Å in **2**, indicating that the intrachain Co–Co interactions might be insignificant. Each chain aligned parallel to the *b* axis in **1** and the *b* + *c* – *a* direction in **2** (Figure S1 in the SI). In both complexes, no short distances to neighboring chains within 6.5 Å were observed, suggesting that the chains are magnetically isolated in the crystalline state. It is noted that the direction of the anisotropic axis due to the cobalt ion, which is assumed to be the direction of oxygen atoms in the **Brhfpip** ligand, has a large angle (62.7 and 64.8° for **1** and 69.1 and 71.4° for **2**) toward the axis of the chain (parts b and e in Figure S1 in the SI).

The crystals were ground, spread over cellophane tape, and used as the sample for SQUID measurement. Photolysis with an argon laser (514 nm and 120 mW) of the diazo groups in complexes **1** and **2** effectively took place in a crystalline state to afford the corresponding cobalt carbene complexes, **1c** and **2c**. The progress of photolysis was followed by the magnetization measurement at 5 K and 5 kOe (Figure S2 in the SI). Upon photolysis, the value of the magnetization steeply increased for 2 h and then increased gradually. After irradiation for ca. 20 h, the degrees of photolysis of the samples were determined to be ca. 88 and 86% for **1** and **2**, respectively, by consumption of IR absorption at 2068 and 2064 cm^{-1} due to the diazo moieties after SQUID measurements.

The direct-current (dc) and alternating-current (ac) magnetic susceptibility data before and after irradiation of the microcrystalline sample of **1** and **2** were collected in the temperature ranges of 1.9–50 and 1.9–30 K, respectively. The $\chi_{\text{mol}}T$ vs *T* plots were obtained at a constant dc field of 5 kOe in the range of 25–50 K and 0.5 kOe below 30 K for **1** and 1 kOe below 30 K for **2** (Figure 2a). Before irradiation of **1**, the $\chi_{\text{mol}}T$ values were nearly constant at 2.0 $\text{cm}^3 \text{K mol}^{-1}$ in the temperature range and were in good agreement with that for a dilute paramagnet, while after irradiation, they increased gradually below 50 K upon cooling, increased abruptly below 20 K, reached a maximum (120 $\text{cm}^3 \text{K mol}^{-1}$) at 12 K, and then decreased. The large maximum value

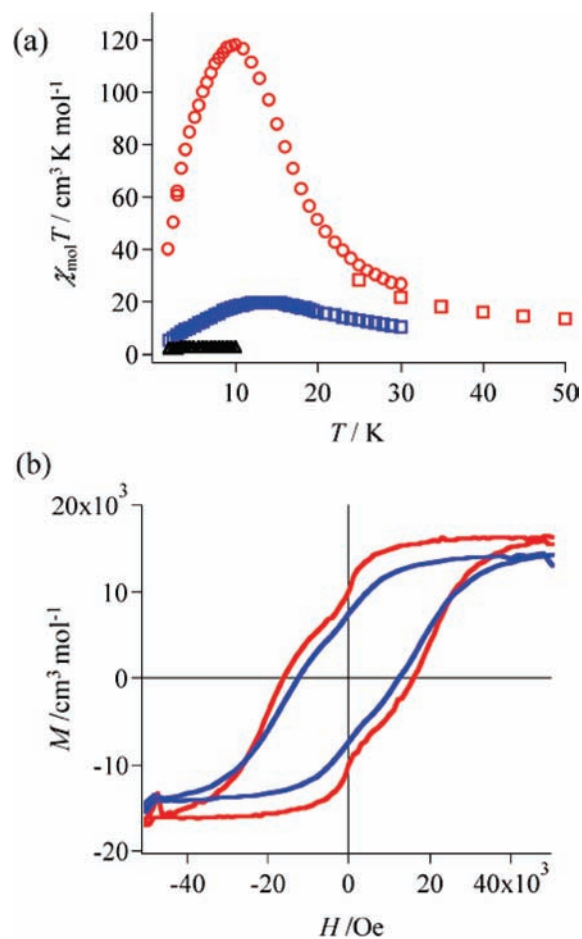


Figure 2. Plots of (a) $\chi_{\text{mol}}T$ vs *T* for **1** (black cross, at 5 kOe), **1c** (red square, at 5 kOe; red circle, at 0.5 kOe), and **2c** (blue square, at 5 kOe) and (b) field dependence of M_{mol} at 1.9 K for **1c** (red) and **2c** (blue).

indicated that the generated carbene and the cobalt ion in the complex units interacted ferromagnetically to form a high-spin chain. The decrease in the χT values below 12 K might be due to an effect of the zero-field-splitting parameter owing to a spin–orbit coupling in the cobalt ion. Complex **2c** also showed a thermal profile on the $\chi_{\text{mol}}T$ vs *T* plot similar to that for **1c** and formed a ferromagnetic chain after irradiation. However, the maximum $\chi_{\text{mol}}T$ value was 20 $\text{cm}^3 \text{K mol}^{-1}$ at 13.5 K, which was one-sixth that for **1c**, indicating that the magnetic correlation length for **2c** below 20 K was shorter than that for **1c** and the ferromagnetic coupling (J_{trans}) between the cobalt ion and the carbene for **2c** was weaker than that (J_{cis}) for **1c**. The difference of magnetic coupling ($J_{\text{cis}} > J_{\text{trans}}$) in the cis and trans isomers was consistent with those in analogous chains of $[\text{Cu- and Mn-}(\text{hfac})_2]_n$.⁴ In addition, the observed difference in the magnitude of the magnetic coupling might be due to the dihedral angles (py–xy) for **1** and **2**. As revealed by the molecular structure analysis, **2** consisted of two units, units A and B, having different dihedral angles. Because the dihedral angles for unit A were close to those for **1**, a weak interaction would be caused by unit B. Therefore, **2c** might be a magnetically alternating chain consisting of units A and B with magnetic exchange coupling constants, J_{trans1} and J_{trans2} ($J_{\text{trans1}} > J_{\text{trans2}} > 0$), respectively (Figure S1f in the SI). Subsequently, the dc magnetizations, M_{mol} , for **1c** and **2c** were measured in the range –50 to +50 kOe and 1.9–3.5 K with

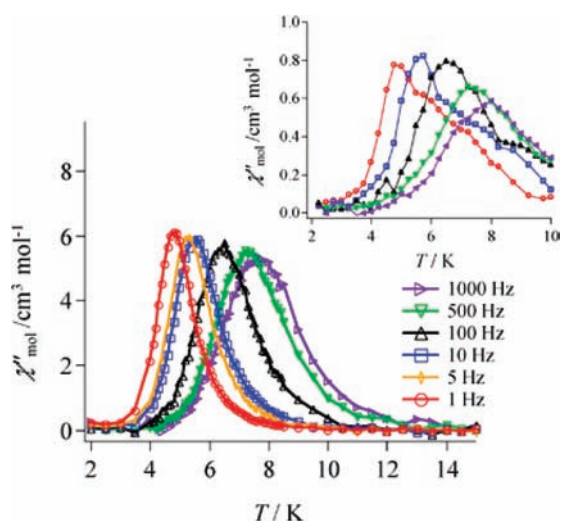


Figure 3. Plots of χ'' vs T of **1c** and **2c** (inset) with a 3.9 Oe ac field oscillating at listed frequencies. The solid lines are visual guides.

a field sweep rate of 0.35 kOe s^{-1} . Interestingly, large hysteresis loops relating to the field were observed below 3.5 K in **1c** and **2c**. The width of the hysteresis loops increased with decreasing temperature (Figure S3 in the SI). The coercive force (H_c) and remnant magnetization (M_r) at 1.9 K for **1c** and **2c** were 20 and 13 kOe and 1.0×10^4 and $7.5 \times 10^3 \text{ cm}^3 \text{ Oe mol}^{-1}$, respectively (Figure 2b). The hysteresis depending on the temperature suggested the formation of a SMM or SCM.

To investigate the slow magnetic relaxation in more detail, ac magnetic susceptibility experiments at a zero dc field with a 3.9 Oe ac field in the frequency of 1–1000 Hz were carried out (Figures 3 and S4 in the SI). Well-resolved χ' and χ'' signals (in-phase and out-of-phase components of ac magnetic susceptibilities, respectively) with a frequency dependence were observed, indicating that the complexes have a slow magnetic relaxation for reorientation of the magnetic moment. The χ'' signals at each frequency showed maxima above 4 K, and the peak-top temperatures shifted lower as the frequency decreased. The thermal profiles of both signals for **1c** and **2c** were similar, but the signal intensities and the shapes of the peaks were largely different. **1c** showed strong signals at each frequency, while **2c** showed weak and broad peaks with a shoulder at the high-temperature side, indicating that the plural components existed. From Arrhenius plots (Figure S5 in the SI), the activation energy for reorientation of the magnetic moment and the preexponential factor, τ_0 , were estimated to be 93 K and $2.4 \times 10^{-9} \text{ s}$ for **1c** and 87 K and $4.4 \times 10^{-9} \text{ s}$ for the major component of **2c**. It is noted that the obtained values of the activation energy were close to each other.

In **1c** and **2c**, the magnetic behaviors observed in dc and ac magnetic susceptibility experiments are typical profiles for SMM and SCM with uniaxial anisotropy. The result that the activation barriers for **1c** and **2c** with different magnitudes of J are comparable may suggest that the magnetic properties of **1c** and **2c** are SMM-like rather than SCM-like. The observed unique magnetic behaviors for **1c** and **2c** chains might be due to the local anisotropic axis at the cobalt ion having the large angle (63 – 71°) toward the axis of the chain.

Quantitative analysis of an analogous heterospin chain using stable N,N -dipyridylaminoxyl and the preparation of a polymeric heterospin complex having the same local anisotropic axis as the direction of the chain are in progress.

ASSOCIATED CONTENT

S Supporting Information. Crystallographic details in CIF format (CCDC 735762 and 735763 for **1** and **2**, respectively), crystal data (Table S1), crystal packing (Figure S1), M vs time plots (Figure S2), M_{mol} vs H below 3.6 K (Figure S3), χ'_{mol} vs T (Figure S4), and Arrhenius plots (Figure S5). This material is available free of charge via the Internet at <http://pubs.acs.org>.

AUTHOR INFORMATION

Corresponding Author

*E-mail: koga@fc.phar.kyushu-u.ac.jp

ACKNOWLEDGMENT

This work was partially supported by the “Nanotechnology Support Project” of the Ministry of Education, Culture, Sports, Science and Technology (MEXT), Japan.

REFERENCES

- (1) Koga, N.; Karasawa, S. *Bull. Chem. Soc. Jpn.* **2005**, *78*, 1384–1400.
- (2) Gatteschi, D.; Sessoli, R.; Villain, J. *Molecular Nanomagnets*; Oxford University Press: New York, 2006.
- (3) (a) Karasawa, S.; Yoshihara, D.; Nakano, M.; Koga, N. *Dalton Trans.* **2008**, 1418–1420. (b) Tobinaga, H.; Suehiro, M.; Ito, T.; Zhou, G.; Karasawa, S.; Koga, N. *Polyhedron* **2007**, *26*, 1905–1911. (c) Karasawa, S.; Zhou, G.; Morikawa, H.; Koga, N. *J. Am. Chem. Soc.* **2003**, *125*, 13676–13677.
- (4) (a) Karasawa, S.; Kumada, H.; Koga, N.; Iwamura, H. *J. Am. Chem. Soc.* **2001**, *123*, 9685–9686. (b) Karasawa, S.; Sano, Y.; Akita, T.; Koga, N.; Itoh, T.; Iwamura, H.; Rabu, P.; Drillon, M. *J. Am. Chem. Soc.* **1998**, *120*, 10080–10087. (c) Sano, Y.; Tanaka, M.; Koga, N.; Matsuda, K.; Iwamura, H.; Rabu, P.; Drillon, M. *J. Am. Chem. Soc.* **1997**, *119*, 8246–8252.
- (5) (a) Miyasaka, H.; Miguel, J.; Yamashita, M.; Clérac, R. *Inorg. Chem.* **2009**, *48*, 3420–3437. (b) Caneschi, A.; Gatteschi, D.; Lalioti, N.; Sangregorio, C.; Sessoli, R.; Ventur, G.; Vindigni, A.; Rettori, A.; Pini, M. G.; Novak, M. A. *Angew. Chem., Int. Ed.* **2001**, *40*, 1760–1763.
- (6) Yoshihara, D.; Karasawa, S.; Koga, N. *J. Am. Chem. Soc.* **2008**, *130*, 10460–10461.
- (7) Liu, Y.-H.; Cheng, Y.-C.; Tung, Y.-L.; Chi, Y.; Chen, Y.-I.; Liu, C.-S.; Peng, S.-M.; Lee, G.-H. *J. Mater. Chem.* **2003**, *13*, 135–142.